Estimation of Intradermal Disposition Kinetics of Drugs: I. Analysis by Compartment Model with Contralateral Tissues

Kazuki Nakayama,[1] Hisae Matsuura,[1] Masahide Asai,[1] Ken-ichi Ogawara,[1] Kazutaka Higaki,[1] and Toshikiro Kimura[1,2]

Received July 13, 1998; accepted September 24, 1998

Purpose. The objectives of dermal application of drugs are not only systemic therapeutics, but also local ones. We would expect its intradermal kinetics to be dependent on its therapeutic purpose. To develop more efficient drugs for local or systemic therapeutics, it will be important to estimate quantitatively the intradermal disposition of drugs applied topically. We tried, therefore, to develop the compartment model to describe the intradermal disposition kinetics after topical application of drugs.

Methods. *In vivo* percutaneous absorption study for antipyrine, a model compound, was performed using rats with tape-stripped skin, using the assumption that the stratum corneum permeability to drugs would be improved enough not to be a rate-limiting process.

Results. To analyze the results obtained, a 4-compartment model, composed of donor cell, viable skin, muscle, and plasma compartments, was applied. Although the fitting lines obtained could describe the concentration-time profiles of antipyrine in each compartment very well, the concentration profiles in the contralateral tissues were extensively overestimated. Therefore, we developed a 6-compartment model which included the viable skin and muscle in the contralateral site, and analyzed the concentration-time curve of each compartment. The fitting curves were in good agreement with the experimental data for all the compartments including the contralateral viable skin and muscle, and thus, this model was recognized to be adequate for the estimation of intradermal kinetics after topical application. Judging from the obtained values of clearance from viable skin to plasma and from viable skin to muscle, about 80% of antipyrine penetrated into viable skin, which suggested it was absorbed into circulating blood and 20% was transported to muscle under viable skin.

Conclusions. Pharmacokinetic analysis using the 6-compartment model would be very useful for the estimation of local and systemic availability after topical application of drugs.

KEY WORDS: intradermal disposition; direct penetration; systemic absorption; stripped skin.

INTRODUCTION

The stratum corneum permeability to drugs could have been enhanced by several approaches such as the usage of lipophilic prodrug (1–3), absorption enhancers (4–6), the formation of complex (7), iontophoresis (8–10), and so on. The enhancers of transdermal absorption have been widely investigated and the promoting mechanisms were elucidated for several promoters (11). Because the stratum corneum is a major barrier for transdermal absorption of many drugs, improvement of transport across the stratum corneum would increase the therapeutic potency of transdermal drug delivery. Since dermal application of drugs is for local therapeutics, as well as systemic therapeutics, transdermal delivery system should be developed according to its therapeutic purpose. This means drugs for systemic therapeutics should be absorbed much more into the blood stream and those for local treatment should penetrate into the underlying deep tissue, e.g., muscle under a viable skin.

There is a controversy concerning the direct penetration into deeper tissues after topical application. It was reported that the distribution of diclofenac (12) and biphenylacetic acid (13) to underlying deep fluid and/or structures occurred mainly via the systemic blood supply. On the other hand, several drugs such as estradiol, progesterone (14), and salicylic acid (15) are reported to be able to penetrate into local deep tissue after topical application.

In the present study, to analyze the intradermal disposition kinetics of a drug after topical application, we designed the experiments that a drug solution would be placed directly on the exposed living epidermis in rats, which enable us to detect the appearance of drugs in underlying deep tissues, to avoid the drug delivery rate-limited by the stratum corneum and to estimate the intradermal kinetics itself. Furthermore, the compartment model composed of 4 or 6 compartments was developed to estimate the direct penetration and the systemic absorption of antipyrine applied topically *in vivo*.

EXPERIMENTAL SECTION

Materials

Antipyrine and aminopyrine, an internal standard, were purchased from Tokyo Chemical Industry Co. (Tokyo, Japan) and Aldrich Chemical Co. (Milwaukee, Wisconsin, USA). All other reagents were of the highest grade commercially available.

Animals

Male Wistar rats weighing 230–270 g were used throughout the present studies and were allowed to freely access standard food and water until studies were carried out. Our investigations were performed after approval by our local ethical committee at Okayama University and in accordance with "Principles of Laboratory Animal Care."

In Vivo Transdermal Absorption Study

Abdominal hair was removed by using 7% thioglycolic acid gel 2 days before performing the absorption study and the stratum corneum was stripped with adhesive tape about twenty times under urethane anesthesia just before starting the absorption study. Under urethane anesthesia, 2 ml of antipyrine solution (5 mM) was applied to the donor cell, of which effective area is 4.91 cm^2, attached on the stripped abdominal skin with Aron Alpha (Toa Chemicals Co., Ltd., Tokyo). After the rats were sacrificed at 0.5, 1, 2, 3, 4, and 7 h, concentrations of

[1] Department of Pharmaceutics, Faculty of Pharmaceutical Sciences, Okayama University, 1-1-1 Tsushima-naka, Okayama 700-8530, Japan.

[2] To whom correspondence should be addressed. (e-mail: kimura@pheasant.pharm.okayama-u.ac.jp)

0724-8741/99/0200-0302$16.00/0

the drug in the donor cell, viable skin, muscle, and plasma were determined.

Tissue Distribution Study After Intravenous Administration

Under urethane anesthesia, after intravenous administration of antipyrine (5 mg/kg), rats were sacrificed at 2, 3, 5, 10, 15, and 30 min and the plasma, abdominal viable skin, and muscle were obtained at each time point. After determining the concentration in each sample, the integration plot (16) was performed to estimate the uptake clearance from plasma to viable skin and muscle. The uptake rate to tissues is described by the following equation:

$$\frac{dX_t}{dt} = CL_{p\text{-}tissue} \cdot C_p \quad (1)$$

where X_t is the amount of antipyrine in tissue at time t, $CL_{p\text{-}tissue}$ and C_p are tissue uptake clearance form plasma and plasma concentration of antipyrine, respectively. The integration of equation (1) gives the equation (2).

$$X_t = CL_{p\text{-}tissue} \cdot AUC_{0\text{-}t} \quad (2)$$

where $AUC_{0\text{-}t}$ indicates the area under the plasma concentration–time curve from 0 to time t. Equation (3) is obtained by division of equation (2) with C_p.

$$\frac{X_t}{C_p} = \frac{CL_{p\text{-}tissue} \cdot AUC_{0\text{-}t}}{C_p} \quad (3)$$

$CL_{p\text{-}tissue}$ is obtained as initial slope by plotting X_t/C_p against $AUC_{0\text{-}t}/C_p$.

In other experiments, after intravenous administration of antipyrine, viable skin, muscle, and plasma were obtained at the elimination phase, and then viable skin to muscle concentration ratio ($Kp_{s/m}$), the viable skin to plasma ($Kp_{s/p}$), and the muscle to plasma ($Kp_{m/p}$) concentration ratios were calculated from their concentrations.

Analytical Procedure

Determination of Antipyrine in Plasma

Plasma was deproteinized with acetonitrile after the addition of internal standard. An aliquot of the supernatant was introduced onto HPLC system described below.

Determination of Antipyrine in Viable Skin and Muscle

Viable skin and muscle was excised at fixed time periods and each of them was placed into the centrifuging tube, where internal standard and 1 ml of 0.5 N NaOH were added. After the tissues were solubilized in the boiling water bath for 30 min, the mixtures were extracted with 6 ml of dichloromethane. The obtained residue after evaporating dichloromethane was dissolved in the mobile phase used in HPLC analysis and injected onto HPLC system. HPLC system consisted of a model LC-6A HPLC pump (Shimadzu, Kyoto, Japan) and a UV detector (SPD-6A; Shimadzu) set at 254 nm. Analytical column was Inertsil $5C_{18}$ (150 × 4.6 mm I.D., GL Sciences, Tokyo). The mobile phase, 20 mM phosphate buffer-methanol (65:35, v/v), was delivered at 1 ml/min. For quantitative calculations, a Shimadzu C-R6A data module was employed. The coefficient of variation (CV) for each standard curve ranged from 0.2 to 5.0% and the squared correlation coefficient was over 0.999.

Pharmacokinetic Analysis

Analysis with 4-Compartment Model

Based on the compartment models composed of donor cell, viable skin, muscle, and plasma as shown in Fig. 1(A), the linear differential equations were obtained as follows.

Donor cell

$$V_d \cdot \frac{dC_d}{dt} = -CL_{d\text{-}vs} \cdot C_d \quad (4)$$

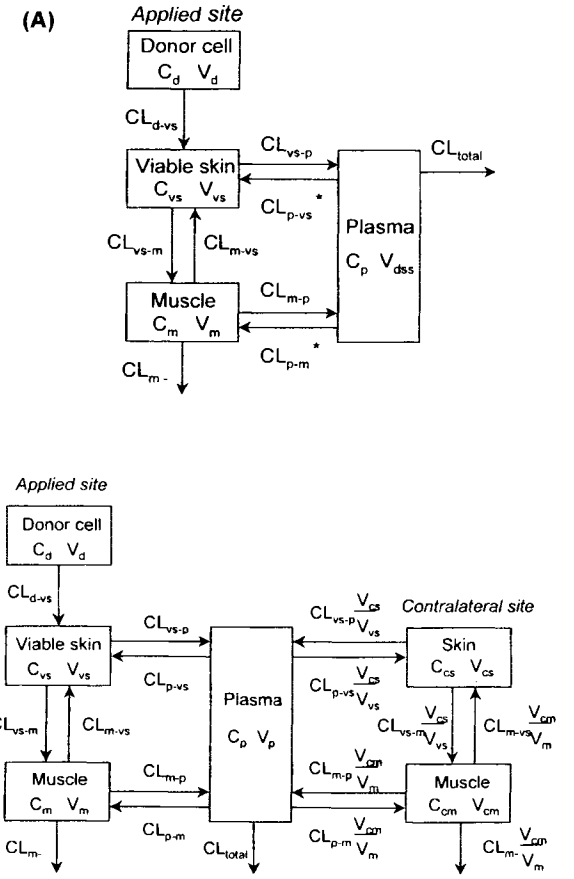

Fig. 1. Pharmacokinetic models describing intradermal kinetics of antipyrine after topical application. (A) and (B) show 4-compartment model and 6-compartment model including contralateral viable skin and muscle, respectively. C and V reveal concentration and distribution volume, respectively. Subscripts of d, vs, m, p, cs and cm reveal the donor cell, viable skin, muscle, plasma, contralateral viable skin and contralateral muscle compartments, respectively. CL indicates the clearance between tissue and tissue or plasma as represented by subscripts. All the clearances except for CL_{total} are calculated as unit of viable skin or muscle mass under application site. * These parameters were obtained from the integration plot.

Viable skin

$$V_{vs} \cdot \frac{dC_{vs}}{dt} = CL_{d\text{-}vs} \cdot C_d + CL_{m\text{-}vs} \cdot C_m + CL_{p\text{-}vs} \cdot C_p - (CL_{vs\text{-}m} + CL_{vs\text{-}p}) \cdot C_{vs} \quad (5)$$

Muscle

$$V_m \cdot \frac{dC_m}{dt} = CL_{vs\text{-}m} \cdot C_{vs} + CL_{p\text{-}m} \cdot C_p - (CL_{m\text{-}vs} + CL_{m\text{-}p} + CL_{m\text{-}}) \cdot C_m \quad (6)$$

Plasma

$$V_p \cdot \frac{dC_p}{dt} = CL_{vs\text{-}p} \cdot C_{vs} + CL_{m\text{-}p} \cdot C_m - (CL_{p\text{-}vs} + CL_{p\text{-}m} + CL_{total}) \cdot C_p \quad (7)$$

where V and C represent the distribution volume and drug concentration in each compartment, respectively. Subscripts of d, vs, m, and p reveal the donor cell, viable skin, muscle, and plasma compartments, respectively. CL indicates the clearance between tissue and tissue or plasma as represented by subscripts.

Drug concentration–time curves were simultaneously fitted with the differential equations described above using MULTI (RUNGE) (17), a nonlinear least-square regression program, and the CL values were obtained. Mean values of each tissue weight, obtained experimentally, were used as a distribution volume of viable skin (0.26 g) or muscle (1.47 g) under the area applied topically.

As CL_{total} and V_p were used, the values of CL_{total} and Vd_{ss} obtained in the intravenous administration study and $CL_{m\text{-}vs}$ were assumed to be $CL_{vs\text{-}m}/Kp_{s/m}$. $Kp_{s/m}$ represents the viable skin to muscle concentration ratio of drug. Furthermore, to augment the precision in the analysis, $CL_{p\text{-}vs}$ and $CL_{p\text{-}m}$ were calculated by the integration plot described above.

Analysis with 6-Compartment Model

We developed 6-compartment model (Fig. 1B) by adding contralateral viable skin and muscle compartments to the 4-compartment model described above. Additional mass balance equations are as follows.

Contralateral viable skin

$$V_{cs} \cdot \frac{dC_{cs}}{dt} = CL_{m\text{-}vs} \cdot \frac{V_{cm}}{V_m} C_{cm} + CL_{p\text{-}vs} \cdot \frac{V_{cs}}{V_{vs}} \cdot C_p - (CL_{vs\text{-}m} + CL_{vs\text{-}p}) \cdot \frac{V_{cs}}{V_{vs}} C_{cs} \quad (8)$$

Contralateral muscle

$$V_{cm} \cdot \frac{dC_{cm}}{dt} = CL_{vs\text{-}m} \cdot \frac{V_{cs}}{V_{vs}} \cdot C_{cs} + CL_{p\text{-}m} \cdot \frac{V_{cm}}{V_m} \cdot C_p - (CL_{m\text{-}vs} + CL_{m\text{-}p} + CL_{m\text{-}}) \cdot \frac{V_{cm}}{V_m} \cdot C_{cm} \quad (9)$$

Plasma

$$V_p \cdot \frac{dC_p}{dt} = CL_{vs\text{-}p} \cdot \left(C_{vs} + \frac{V_{cs}}{V_{vs}} \cdot C_{cs}\right) + CL_{m\text{-}p} \cdot \left(C_m + \frac{V_{cm}}{V_m} \cdot C_{cm}\right) - \left(CL_{p\text{-}vs} + CL_{p\text{-}m} + CL_{p\text{-}vs} \cdot \frac{V_{cs}}{V_{vs}} + CL_{p\text{-}m} \cdot \frac{V_{cm}}{V_m} + CL_{total}\right) \cdot C_p \quad (10)$$

where the subscripts of cs and cm represent contralateral viable skin and contralateral muscle, respectively. As all the clearances except for CL_{total} are calculated as unit of viable skin or muscle mass under application site, the correction by distribution volume is necessary as described above to estimate the substantial value of clearance for contralateral tissues. Tissue concentration–time curves of 6 compartments were fitted with differential equations (4)–(6), (8)–(10) using MULTI (RUNGE). In this model analysis, it was assumed that (a) contralateral viable skin and muscle represent all the those except the applied site. (b) CL (per g tissue) between plasma and any tissue is equal without distinction of applied or non-applied sites. (c) Vp can be obtained by the following equation:

$$V_p = Vd_{ss} - Kp_{s/p} \cdot V_{cs} - Kp_{m/p} \cdot V_{cm} \quad (11)$$

where $Kp_{s/p}$ and $Kp_{m/p}$ represent the viable skin and muscle to plasma concentration ratios of drug, respectively, and the values of V_{cs} and V_{cm} were assumed to be 43.5 g and 125 g (18), respectively.

In both model analyses, the final fitting was deemed acceptable based on the regression goodness-of-fit criteria, the Akaike's information criteria (19).

RESULTS AND DISCUSSION

Dermal and transdermal delivery of drugs has at least three purposes as follows: (i) improvement of systemic therapeutics, (ii) treatment of the upper part of skin, and (iii) treatment of the deeper tissues, such as dermis and muscle. For the development of the efficient delivery system according to each therapeutic purpose, the understanding and the control of the intradermal disposition kinetics of drugs must be important in addition to the enhanced permeability of stratum corneum.

In the present study, to analyze the intradermal disposition kinetics of antipyrine, 4-compartment model was developed first as shown in Fig. 1(A), in which viable skin represents living epidermis and dermis. In this model analysis, we used the values of $CL_{p\text{-}vs}$ and $CL_{p\text{-}m}$ obtained from the integration plots because we had inquired about less incredibility in these parameters. Figure 2 shows the integration plots of viable skin and muscle. The ratio of drug amount in each tissue to the plasma concentration was plotted against the ratio of AUC to the plasma concentration at each time. Clearance values were calculated by using the initial three points showing good linearity because the back diffusion from each tissue to plasma could be neglected in such early periods of time and so the uptake clearance from plasma to each tissue can be estimated precisely

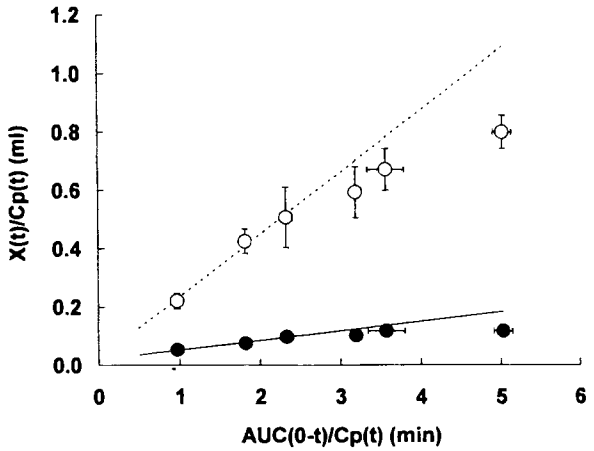

Fig. 2. Estimation of antipyrine transport to viable skin and muscle from systemic circulation after intravenous administration (Integration plot). Results are expressed as the mean with a vertical and a horizontal bar showing the S.E. of more than 3 experiments. The initial straight lines, obtained by the least squares regression, indicate the uptake clearance. Key: —●—, viable skin (slope, 0.0327 ml/min/tissue; r = 0.989); --○--, muscle (slope, 0.2127 ml/min/tissue; r = 0.995).

(16). The substantial value of $CL_{p\text{-}m}$ was suggested to be much larger than that of $CL_{p\text{-}vs}$ (Table 1). The values of Kp were obtained as follows: $Kp_{s/p}$, 0.748 ± 0.008; $Kp_{m/p}$, 0.872 ± 0.014; $Kp_{s/m}$, 0.859 ± 0.022 (the mean ± S.E. of 4 experiments).

Figure 3 represents the observed data and the fitting curves obtained by the analysis using 4-compartment model and the pharmacokinetic parameters were summarized in Table 1. Taking into consideration the values of $CL_{vs\text{-}m}$ and $CL_{vs\text{-}p}$, about 16% of antipyrine in viable skin can directly penetrate into the muscle layer below the living epidermis (topical application site). These lines seem to describe the intradermal kinetics of antipyrine well, judging from the results in Fig. 3. The concentrations of antipyrine in the contralateral muscle, however, were recognized to be overestimated in this analysis (Fig. 4). The concentration profile in the contralateral muscle was calculated using the parameters obtained by 4-compartment model analysis and the great discrepancy between the observed data and predicted curve suggests the incredibility of the results by 4-compatment model analysis.

Therefore, we added the contralateral viable skin and muscle compartments to the 4-compartment model (Fig. 1(B)) and performed the simultaneous fitting for 6 fluids and/or tissues (Fig. 5) based on the 6-compartment model. The calculated lines could very well describe the plasma concentration profile and the intradermal kinetics including the contralateral tissues. The values of clearances thus obtained were listed in Table 1. As compared with those by 4-compartment model, there was a quite difference only in $CL_{p\text{-}m}$ between the two models. The overestimation of $CL_{p\text{-}m}$ by 4-compartment model analysis should be substantially attributed to the integration plot, but the reason for this overestimation has been unknown so far. Although $CL_{m\text{-}}$ is less credible, other important clearances obtained will be highly credible, judging from the small values of S.D. Especially, as for $CL_{p\text{-}m}$ and $CL_{m\text{-}p}$ their propriety is testified by the fact that the ratio of $CL_{p\text{-}m}$ to $CL_{m\text{-}p}$ (1.08) is much more comparable to $Kp_{m/p}$ value (0.872) than the ratio (4.36) obtained by 4-compartment model analysis, because the ratio as mentioned above may be equal to the $Kp_{m/p}$ value at a steady state.

The values of $CL_{vs\text{-}m}$ and $CL_{vs\text{-}p}$ could be indices for the efficiency of systemic delivery or local delivery and these values indicate about 20% of antipyrine in the viable skin after topical application can directly penetrate into the muscle layer below the application site. Singh and Roberts estimated their contributions in removing salicylic acid from several tissues and suggested that 33% of salicylic acid in the dermis should be removed by direct penetration into the deeper tissues (15). Although they assumed the rate of blood flow in each tissue to be a clearance by blood circulation, we calculated $CL_{vs\text{-}p}$ for antipyrine, by which we estimated their contributions. The removing clearance by blood circulation would also be dependent on the physicochemical characteristics of drugs to some extent and different drugs would have different values of the clearance. Furthermore, we estimated the contributions of direct penetration and transport from systemic circulation to the muscular distribution of antipyrine after topical application. As shown in Fig. 6, it was suggested antipyrine in the muscle layer below the application site should be largely attributed to the direct penetration. The values of AUC calculated according to the trapezoidal rule (AUC_{direct}, 559.1; AUC_{system}, 83.2 nmol·h/ml) indicate that 87% of AUC can be derived from the direct penetration. Although the contribution of the direct penetration is suggested to be dependent on the drugs applied topically (12–15), our present results clearly indicate significant amounts of antipyrine should penetrate into the muscle layer, especially at muscle layers below the applied site; almost all the drug should be ascribed to direct penetration. Singh and Roberts reported fractional contribution of direct penetration and of blood supply in determining the flux for salicylic acid (15) and

Table 1. Pharmacokinetic Parameters Describing Intradermal Kinetics of Antipyrine After Topical Application

Pharmacokinetic models	Pharmacokinetic parameters						
	$CL_{d\text{-}vs}$ (ml/h)	$CL_{vs\text{-}m}$ (ml/h)	$CL_{vs\text{-}p}$ (ml/h)	$CL_{p\text{-}vs}$ (ml/h)	$CL_{m\text{-}p}$ (ml/h)	$CL_{p\text{-}m}$ (ml/h)	$CL_{m\text{-}}$ (ml/h)
4-compartment model	0.343[a] ± 0.016	0.458 ± 0.005	2.430 ± 0.004	1.961[b]	2.929 ± 0.118	12.764[b]	0.003 ± 65.713
6-compartment model	0.343[a] ± 0.016	0.556 ± 0.009	2.320 ± 0.006	2.533 ± 0.023	2.441 ± 0.054	2.648 ± 0.055	0.001 ± 1.825

Note: Pharmacokinetic parameters were expressed with SD. They were obtained by fitting the differential equations based on each pharmacokinetic model to the observed mean data using MULTI (RUNGE).

[a] The values of $CL_{d\text{-}vs}$ was calculated independently and used as a constant value in the fitting analysis described above.

[b] These parameters were obtained from the integration plot as follows: the slope obtained in Figure 2 (×60).

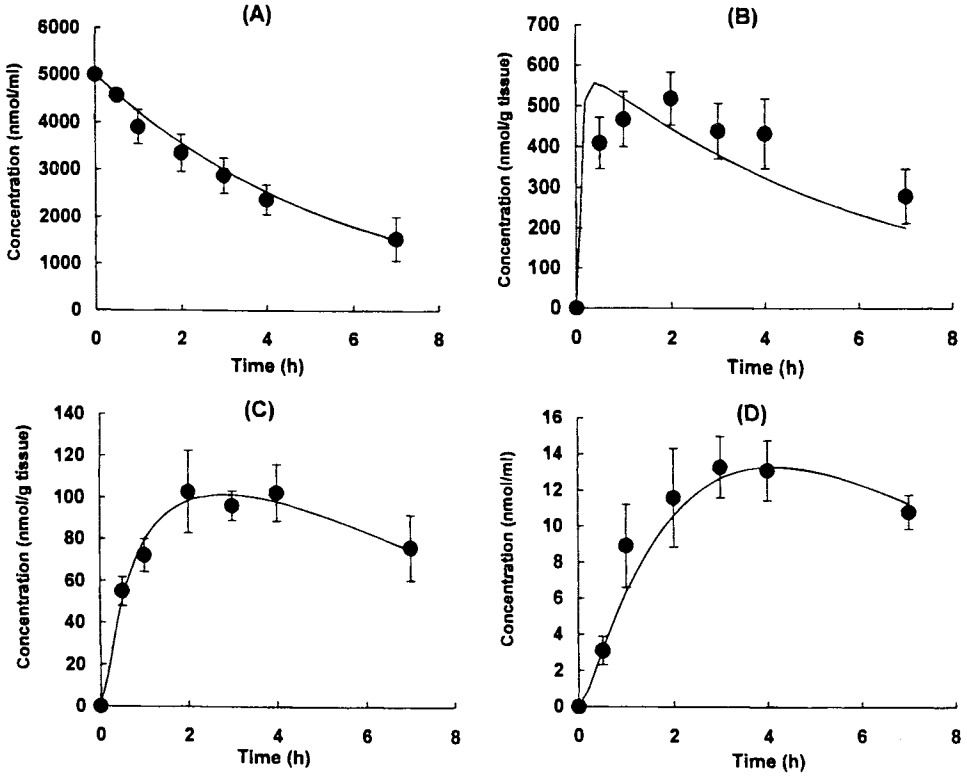

Fig. 3. Pharmacokinetic analysis of intradermal disposition of antipyrine using 4-compartment model. (A), (B), (C) and (D) represent Donor cell, Viable skin, Muscle and Plasma, respectively. Results are expressed as the mean with a vertical bar showing the S.E. of more than 3 experiments. Solid lines represent the obtained fitting curves.

lidocaine (20) in the tissues below the applied site. In the case of the two drugs, the direct penetration is extensively dominant in the upper layer and its contribution decreases with increasing depth. In deep muscle, the deepest layer they investigated, 62% of salicylic acid is attributed to the blood supply. On the other hand, they indicated 70% of lidocaine was still supplied by direct penetration in the deepest layer. In the present study, we assumed the muscle layer to be a single compartment and estimated the concentration in muscle up to a depth of about 3 mm including almost all the layers below viable skin at abdominal side in rats. Therefore, we can only compare the viable skin layer with the muscle layer in the present study. To perform the comparison as mentioned above, the amount of antipyrine supplied by direct penetration or systemic circulation was calculated according to the following equations: $A_{d\text{-}vs} = CL_{d\text{-}vs} \cdot AUC_d$ (1280 μg); $A_{p\text{-}vs} = CL_{p\text{-}vs} \cdot AUC_p$ (36 μg); $A_{vs\text{-}m} = CL_{vs\text{-}p} \cdot AUC_{vs}$ (293 μg), $A_{p\text{-}m} = CL_{p\text{-}m} \cdot AUC_p$ (38 μg). "A" represents the amount of antipyrine and the subscripts represent the same elements as described in the Experimental section. The fractional contribution of direct penetration obtained from the results described above is about 97% or 89% in the viable skin or muscle, respectively, suggesting the disposition of antipyrine to the deeper tissue is similar to that of lidocaine regardless of the difference in physicochemical property between the two drugs. The larger contribution of the direct penetration to deeper tissue for lidocaine than for salicylic acid are suggested to be dependent on its binding less to the tissue. The free fraction of antipyrine determined preliminarily is 0.96 using 10% homogenate of viable skin, which may be responsible for its greater penetration to the deeper muscle. However, the lipophilicity of drugs may not have anything to do with the contribution of their direct penetration, because there is a large difference in lipophilicity between lidocaine (lop P = 1.64 (20)) and antipyrine (log P = 0.39). Although Singh and Roberts suggested small molecules allowing the

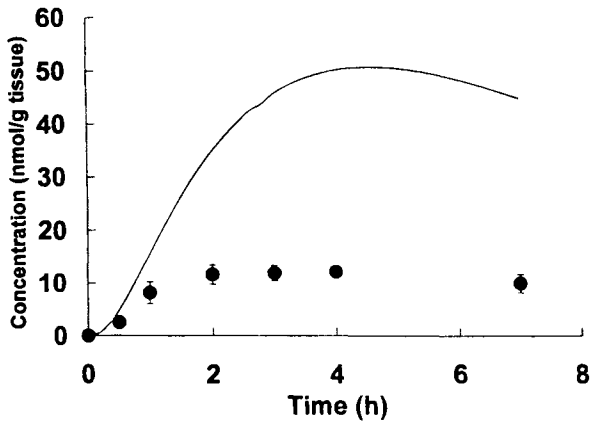

Fig. 4. Overestimation of antipyrine concentration in contralateral muscle by 4-compatment model analysis. Results are expressed as the mean with a vertical bar showing the S.E. of more than three experiments. The bars are hidden behind symbols. Solid line was described by using the parameters obtained by 4-compartment model analysis.

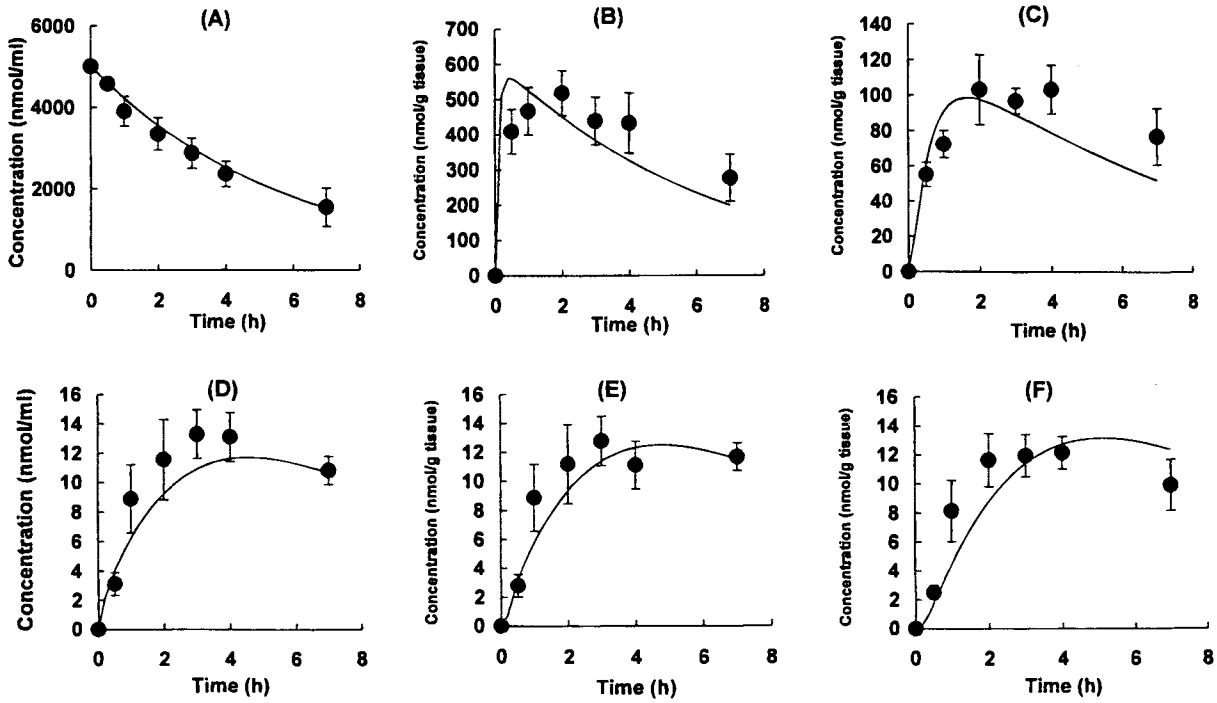

Fig. 5. Pharmacokinetic analysis of intradermal disposition of antipyrine using 6-compartment model. (A) Donor cell, (B) Viable skin, (C) Muscle, (D) Plasma, (E) Contralateral viable skin, (F) Contralateral muscle. Results are expressed as the mean with a vertical bar showing the S.E. of more than 3 experiments. Solid lines represent the obtained fitting curves.

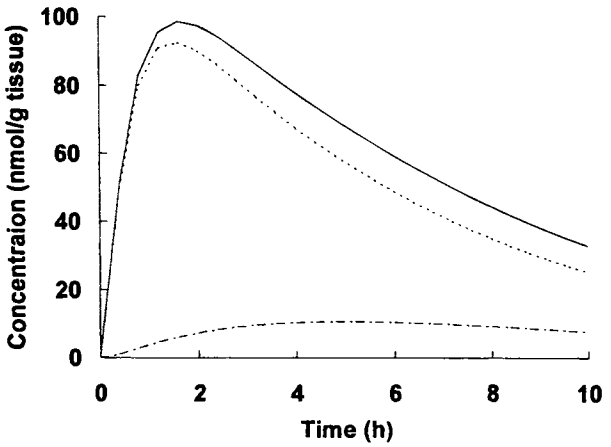

Fig. 6. Evaluation of direct penetration and transport from systemic circulation to muscle layer below the application site. Simulation curves were described using the parameters obtained by 6-compartment model analysis. Key: ——, total concentration; -----, the concentration due to direct penetration; ——, the concentration due to systemic circulation.

drugs to diffuse easily should be an important factor (21), in truth, further studies are needed to elucidate the factors determining intradermal disposition of drugs applied topically.

In conclusion, we developed the pharmacokinetic model describing the intradermal disposition of drugs applied topically and could evaluate the fractional contribution of the direct penetration and the blood supply to the deeper muscle layer below the applied site.

REFERENCES

1. M. Hashida, E. Mukai, T. Kimura, and H. Sezaki. Enhanced delivery of mitomycin C prodrugs through the skin. *J. Pharm. Pharmacol.* **37**:542–544 (1985).
2. S. Y. Chan and A. Li Wan Po. Prodrugs for dermal delivery. *Int. J. Pharm.* **55**:1–16 (1989).
3. F. Palagiano, L. Arenare, F. Barbato, M. I. La Rotonda, F. Quaglia, F. P. Bonina, L. Montenegro, and P. de Caprariis. In vitro and in vivo evaluation of terpenoid esters of indomethacin as dermal prodrugs. *Int. J. Pharm.* **149**:171–182 (1997).
4. A. C. Williams and B. W. Barry. Skin absorption enhancers. *Crit. Rev. Ther. Drug Carrier Sys.* **9**:305–353 (1992).
5. N. Ohara, K. Takayama, Y. Machida, and T. Nagai. Combined effect of d-limonene and temperature on the skin permeation of ketoprofen. *Int. J. Pharm.* **105**:31–38 (1994).
6. Y. Nakamura, K. Takayama, K. Higashiyama, T. Suzuki, and T. Nagai. Promoting effect of *O*-ethylmenthol on the percutaneous absorption of ketoprofen. *Int. J. Pharm.* **145**:29–36 (1996).
7. J. Hadgraft, K. A. Walters, and P. K. Wotton. Facilitated transport of sodium salicylate across an artificial lipid membrane by Azone. *J. Pharm. Pharmacol.* **37**:725–727 (1985).
8. Y. W. Chien, O. Siddiqui, W. M. Shi, P. Lelawongs, and J. C. Liu. Direct current iontophoretic transdermal delivery of peptide and protein drugs. *J. Pharm. Sci.* **78**:376–383 (1989).
9. P. Singh, M. S. Roberts, and H. I. Maibach. Modelling of plasma levels of drugs following transdermal iontophoresis. *J. Contr. Rel.* **33**:293–298 (1995).
10. J. E. Riviere and M. C. Heit. Electrically-assisted transdermal drug delivery. *Pharm. Res.* **14**:687–697 (1997).
11. B. W. Barry. Lipid-protein-partitioning theory of skin penetration enhancement. *J. Contr. Rel.* **15**:237–248 (1991).
12. J. Radermacher, D. Jentsch, M. A. Scholl, T. Lustinetz, and J. C. Frolich. Diclofenac concentrations in synovial fluid and plasma after cutaneous application in inflammatory and degenerative joint disease. *Br. J. Clin. Pharmacol.* **31**:401–418 (1991).
13. M. Dawson, C. M. McGee, J. H. Vine, P. Nash, T. R. Watson,

and P. M. Brooks. The disposition of biphenylacetic acid following topical application. *Eur. J. Clin. Pharmacol.* **33**:639–642 (1988).

14. J. P. Marty, R. H. Guy, and H. I. Maibach. I. Percutaneous penetration as a method of delivery to muscle and other tissues. In R. L. Bronaugh and H. I. Maibach (eds.), *Percutaneous Absorption: Mechanisms, Methodology, Drug Delivery* (2nd ed.), Marcel Dekker, New York, 1989, pp. 511–529.
15. P. Singh and M. S. Roberts. Dermal and underlying tissue pharmacokinetics of salicylic acid after topical application. *J. Pharmacokinet. Biopharm.* **21**:337–373 (1993).
16. M. Yamazaki, H. Suzuki, M. Hanano, T. Tokui, T. Komai, and Y. Sugiyama. Na^+-independent multispecific anion transporter mediates active transport of pravastatin into rat liver. *Am. J. Physiol.* **264**:G36–G44 (1993).
17. K. Yamaoka and T. Nakagawa. A nonlinear least squares program based on differential equations, MULTI(RUNGE), for microcomputers. *J. Pharmacobio-Dyn.* **6**:595–606 (1983).
18. T. Iga, Y. Sawada, and Y. Sugiyama. Physiological pharmacokinetics: the method of parameter calculation. In M. Hanano, T. Umemura, and T. Iga (eds.), *Applied Pharmacokinetics: Theory and Experiments*, Soft Science Inc., Tokyo, 1985, pp. 431–473.
19. K. Yamaoka, T. Nakagawa, and T. Uno. Application of Akaike's information criterion (AIC) in the evaluation of linear pharmacokinetic equations. *J. Pharmacokinet. Biopharm.* **6**:165–175 (1978).
20. P. Singh and M. S. Roberts. Dermal and underlying tissue pharmacokinetics of lidocaine after topical application. *J. Pharm. Sci.* **83**:774–782 (1994).
21. P. Singh and M. S. Roberts. Local deep tissue penetration of compounds after dermal application: structure-tissue penetration relationships. *J. Pharmacol. Exp. Ther.* **279**:908–917 (1996).